DOI: 10.1002/chem.200801074

Is there an Intrinsic Limit to the Size of 2D Supracrystals Built from Weakly Interacting Nanoparticles?

Christian Amatore*[a]

Abstract: This work establishes that an extremely stringent, but dismissed thermodynamic condition governs the size of perfect 2D supracrystals that consist of weakly interacting nanoparticles. This severe condition is ultimately imposed by the large modulus of the negative entropy, which accumulates in any large defect-free (or defectless) crystal, owing to the high demand for the precise ordering of its arrayed elements. This thermodynamic toll is especially difficult to compensate for when interaction enthalpies within the lattice and its underlying substrate are weak, as is required for these arrays, which are valuable for innovative applications such as optics, electronics and magnetism. This constraint is formulated here by a simple scale law which predicts the maximum size achievable for 2D supracrystals as a function of their surface and edge enthalpies. This scale law analysis is ultimately based on the recognition that the modulus of entropic contributions grows faster (as $\ln(N_0!)$ in which N_0 is the number of perfectly arrayed particles) than that of enthalpic ones ($\propto N_0$) when the size of any perfectly ordered structure increases. Hence, disorder must be introduced into the network to relax the entropic demand to allow sufficient stability. This intrinsic characteristic is shown to be extremely prohibitory if the enthalpic interactions between the arranged objects are close to the thermal quantum, as is imposed for the applications mentioned above. To substantiate this concept, we have evaluated the thermodynamics of 2D supracrystals composed of nanoparticles arranged into the most common crystallographic arrays (square, *c*, square-centered, *cc*, or hexagonal, *hex*, lattices). The essentially identical results obtained for these there lattices establish that the scale law developed here is valid for most realistic lattices.

Keywords: 2D arrays · nanoparticles · supracrystals · thermodynamics

Introduction

Intense research efforts are being devoted to the synthesis of perfect silicon-supported flat macroscopic 2D supracrystals composed of nanometric metal nanoparticles. Based on specific electromagnetic characteristics such arrays have been predicted to offer several innovative applications in optics, electronics, and magnetism.[1] However, central to the expected future devices is the requirement that the nanoparticles composing such arrays should have minimal electronic interactions between themselves or with the base substrate on which these 2D supracrystals are grown.[1] A technological requirement for mass production of effective devices based on this concept is that the 2D supracrystals must be defect-free while extending over significant areas (i.e., $\approx 1\ cm^2$). Even if the first requirement is certainly achieved, the second one appears extremely difficult to reach.[2–4]

Self-organization, i.e., involving weak enthalpic interactions between arrayed objects (e.g., such as van der Waals forces),[2,3] appears to be the present method of choice for constructing 2D supracrystals with the characteristics described above. However, though this is one of the basic interactions retained by nature to create 2D or 3D assemblies (e.g., viruses), and despite the importance and increasing number of synthetic works relying on this concept for producing high quality 2D supracrystals of metal nanoparticles,[2,4] it appears that the best defect-free 2D-single-crystal arrays reported up-to-date are generally far from meeting the minimum sizes required for any practical industrial applications. In practice, the nanoparticles arrange at most in neat defect-less micrometric subdomains whose juxtaposition covers the base substrate,[2–4] a prohibitory situation.[1]

Present size limits cannot be ascribed to distortions introduced by dispersion of the nanoparticle sizes composing the

[a] Dr. C. Amatore
UMR CNRS 8640 "PASTEUR"
and LIA CNRS XiamENS "NanoBioChem"
Département de Chimie, Ecole Normale Supérieure
Université Pierre et Marie Curie-Paris 6
24 rue Lhomond, 75231 Paris Cedex 05 (France)
Fax: (+33) 144-323-863
E-mail: christian.amatore@ens.fr

2D supracrystals, as this has been under appropriate control already for several years.[5] It seems implicitly assumed by many authors that the origin of the defects that limit the size of 2D-single crystals is mostly related to the complexity of the delicate interplay between growth kinetics and transport of nanoparticles to the crystallization sites, as well as to the control of nucleation rates, so that great efforts are being devoted to controlling growth kinetics through different strategies adapted to different contexts.[2–9]

Kinetics is certainly a key issue as is very well known for the growth of any single crystals. This has been demonstrated and rationalized in great detail for 2D supracrystals by Chaikin,[6] Kramer,[7] Nelson,[8] and Ertl[9] in a series of seminal works. However, we wish here to examine the problem from a different angle. Namely, even if such kinetic problems could be brought under perfect control by adequate synthetic strategies, would that be sufficient to solve the problem of manufacturing large size 2D supracrystals of weakly interacting nanoparticles?

In evaluating the potential stability of 2D crystals only strict enthalpic contributions (H) are generally considered.[3,10] However, if the magnitude of the enthalpy of a supracrystal grows as the number, N_0, of arrayed particles, the entropic demand (S) grows faster than the number of arrayed particles reflecting the increasing demand for order when more and more nanoparticles are assembled.

Whenever the absolute value of the enthalpy per nanoparticle (in the Madelung sense, i.e., including all interactions: between the particles themselves, with the underlying substrate and accounting for any change incurred by the base substrate, owing to the presence of the nanoparticle coverage; however this does not include the enthalpy of formation of the nanoparticles from their atomic components) is much larger than the thermal quantum, k_BT, as occurs for example in classical inorganic crystals (e.g., NaCl, quartz, diamond, etc.) the overall negative enthalpy of the arrayed particles compensates easily for the large order demand created when the crystal size becomes excessively large. However, this may not be the case if the enthalpy per nanoparticle needs to be small as is required for the applications described above.

Under such delicate conditions (i.e., when the enthalpic drive is poor), the system must find ways to relax its too demanding order to achieve any thermodynamic stability. This necessarily corresponds to the spontaneous creation of several types of defects and dislocations. Such states are generally associated with weaker enthalpies than those of the perfectly arrayed elements in the crystalline network, but they may help to lower the overall Gibbs free energies (i.e., free enthalpies) because the corresponding amount of disorder introduced in the crystal corresponds to positive entropic contributions relative to a perfect array. This view seems to justify qualitatively the segregation of would-be macroscopically perfect 2D supracrystals into a series of juxtaposed micrometric perfectly ordered subdomains.[2–4]

In the following, we wish to examine if a would-be perfect single-domain 2D supracrystal (that we take everywhere as the reference state even if it may not actually exist experimentally) may experience a thermodynamic drive for rearranging into subdomains so as to decrease its primitive too-high order and minimize locally its overall Gibbs energy (in this work we use the term "Gibbs free energy" to represent the "standard free enthalpy", i.e., the thermodynamic state function $G^0=H^0-TS^0$ in which T is the absolute temperature, H^0 the standard enthalpy, and S^0 the standard entropy).

For this reason we do not need to specify the initial state in which the nanoparticles are before they assemble onto the substrate. Because our thermodynamic reference state is a perfectly arrayed 2D supracystal, the property that we wish to establish here is independent of the initial status of the nanoparticles before they assemble into the array. It only determines the most favorable ordered structure of the assembly, if any one may be formed. By all means, the present analysis does not imply that such most stable state has any intrinsic thermodynamic stability, since this depends on external factors defining the system before it assembles.

From a strict point of view the very chemical nature of defects matters. However, spontaneous formation of dislocations defining perfectly organized subdomains whose juxtaposition fully covers the underlying substrate is often reported for actual 2D supracrystals of the type envisioned here.[1–4] Keeping in view that the ultimate synthetic goal is the possibility of manufacturing defectless 2D supracrystals with feebly interacting objects, we propose to consider only this single type of defect. In doing so we certainly particularize a single mode of relaxing the too large entropic demand. On the other hand, this choice is representative of many experimental situations[1–4] and is particularly helpful in evaluating the compromise between enthalpic and entropic contributions. In a real case the thermodynamic constraint that we ascribe to a single specific type of defect may be "shared" by the presence of other defects, e.g., such as those identified and thoroughly investigated by Chaikin,[6] Kramer,[7] and Nelson[8] or other specific ones, e.g., as hexatic defects,[10,11] or any others. Yet, by essence, such defects will distribute over the whole assembly and prevent anyway the use of the ensuing 2D supracrystals for the presently targeted innovative applications in optics, electronics and magnetism.[1] Hence, our analysis is aimed to provide a minimal thermodynamic requirement for 2D supracrystals prone to such type of applications. For the same reason we consider only statistical Boltzmannian entropic contributions[13a] and we do not specify the exact chemical nature of the interactions of nanoparticles with its neighbors or with the base surface, nor the exact changes in surface and edge tension energies experienced by the base substrate.

For the sake of pedagogical presentation we chose to present in the main text a thorough analysis considering specifically squared crystallographic arrangements (c) since this simplifies the formulations while keeping intact its principle (note that in all this work, we use the classical notations for 3D lattices, *c*, *cc*, or *hex*, though we investigate 2D lattices). In selecting a squared lattice to illustrate the present scaling law analysis, we fully appreciate that generally the experi-

mental supracrystals arrange into centered squared (*cc*) or hexagonal (*hex*) arrays,[2,4] owing to the maximization of density and interactions. For this reason we report also the final outcomes of our approach for *cc* and *hex* 2D supracrystals in the main text, but fully disclose their analyses in the Appendix. Regardless, the problem that we examine hereafter does not significantly depend on the precise crystallographic lattice type, but rather on essential scale factors that are related only to the number of particles arranged in 2D supracrystals as soon as this number is large enough for any realistic application such as those envisioned here.[1]

Theory

Defining a general scaling law for 2D-supracystals: Let us consider a perfectly flat 2D wafer of surface area A_0 covered by a perfectly ordered 2D array consisting of N_0 nanoparticles of individual radius r_p. This is taken as the thermodynamic reference state without presuming that such an array may actually be formed even transiently. Let us assume that such perfect array may evolve so that, although still covering the same surface of the wafer with the same number of particles,[14] it gives rise to a series of extremely thin dislocations that separate the initial continuous 2D crystal in a juxtaposed series of N_D perfectly ordered 2D subdomains consisting each of 2D supracrystals (see Figure 1). Such composite

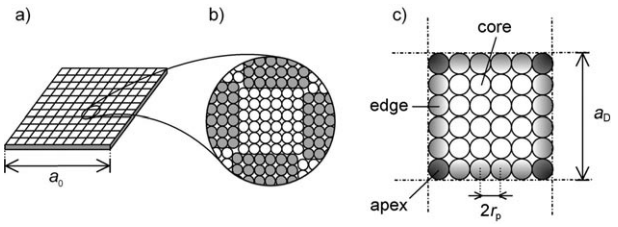

Figure 1. Schematic representation of a wafer covered by independent domains consisting of 2D supracrystals (this is illustrated for squared (*c*) arrangements). a) View of a squared-wafer covered with a squared arrangement of N_D identical perfect 2D supracrystalline juxtaposed subdomains. b) Schematic illustration of the arrangement of distinct single crystals. c) Schematic view defining the different classes of nanoparticles in any subdomain.

supracrystals have indeed been frequently reported experimentally when enthalpies of interactions in the array are weak.[1–4] In this view, the single 2D supracrystal used as our reference state is represented by $N_D=1$ to represent that a single perfect domain is achieved. Our first aim here is to evaluate the Gibbs energy variation, $\Delta G_{N_D}^{N_0}=G_{N_D}^{N_0}-G_{N_D=1}^{N_0}$, experienced if a single domain splits into N_D subdomains. This will serve to examine afterwards if a particular value of N_D confers a local stability on a particular component of this family, if $\Delta G_{N_D}^{N_0}$ experiences a single minimum when N_D varies between unity and its limit for a fully random array (i.e., $N_D \rightarrow N_0$).

The present model is not aimed to solve any specific situation (as performed in previous seminal works),[6–9] but to propose a general scaling law that may result useful to synthetic chemists for designing new strategies for manufacturing large 2D supracrystals consisting of weakly bound nanoparticles. Its root consists in remarking that the main enthalpic drive in creating a perfect 2D supracystal is approximately proportional to the cumulative surface area of the ordered domains, taking into account core and edge interactions, although the entropic contribution consists of two terms. One is negative and features the high "order demand", owing to the population of perfectly arrayed particles. The second one is positive and represents the "disorder allowance" within the composite supracrystal; this includes the defects (misplaced particles, defects, absence of particles). We assume that for the minimization of energy these defects assemble into chain boundaries defining the subdomains.[6a] In this regard, we exclude the possibility that these boundaries may result fractal to any significant degree, even if they are possibly crossing (see Figure 1) to delimit ordered subdomains. It is essential to our analysis that the boundaries keep a dimensionality equal or closely equivalent to that of a length.

If a general scaling law exists to define the most thermodynamically stable arrangement, the number N_D of subdomains for a given number N_0 of nanoparticles, it is intuitively expected to depend on the specific lattice (e.g., *c*, *cc*, *hex*) assumed by the nanoparticles. However, from the general theoretical point of view developed here, the precise nature of the crystallographic array influences the following theoretical description only through the introduction of specific geometrical factors whose values are commensurable to unity (see below and Appendix). For this reason we will pursue our analysis by considering squared supra-crystallographic arrangements (*c*) of nanoparticles (Figure 1c), as this is the 2D-crystallographic arrangement that leads to the simplest intermediate formulations while keeping intact the general principle and outcome of the present model (see below). The Appendix presents the same analyses for squared centered (*cc*) and hexagonal arrays (*hex*), hence validating quantitatively this choice for simplification of our presentation.

Finally, we wish to recall that when $N_D \gg 1$ it is probable that a distribution of clusters sizes (presenting a distribution of their surface areas A_D) should be observed. However, as will become evident in the following we are interested in the situation when $N_D=1$, as this is the one which matters for any practical application.[1] Therefore, for keeping a general character to our analysis while simplifying its presentation we will consider that all subdomains are identical (that the distribution of A_D is close to a Dirac delta function). In doing so we certainly minimize the entropic contributions related to disorder by minimizing ex abrupto one configurational component.[12] Yet, as the final outcome of our approach is to produce a scaling law that describes the condition required for obtaining $N_D=1$, this assumption is not critical for the final outcome of our theoretical model.

Let then the common lateral dimension of each single defect-free 2D-supracrystal square domain be a_D (Fig-

ure 1c), and that of the composite 2D supracrystal be a_0 (Figure 1a). To proceed let us introduce first the following parameters that transcribe the above geometrical descriptions into dimensionless values. Equation (1) is the overall number of particles assembled onto the 2D wafer:[15]

$$N_0 = \frac{A_0}{4r_p^2} = \left(\frac{a_0}{2r_p}\right)^2 \tag{1}$$

Equation (2) is the number of identical perfect 2D domains:

$$N_D = \frac{A_0}{A_D} = \left(\frac{a_0}{a_D}\right)^2 \tag{2}$$

Equation (3) is the number of particles in each subdomain:

$$N_p = \left(\frac{a_D}{2r_p}\right)^2 \tag{3}$$

Each 2D subdomain (Figure 1c) includes N_p^{core} "core" nanoparticles, i.e., located within the subdomain core, N_p^{edge} "edge" particles, lined along the domain edge and experiencing a relative destabilization, owing to edge effects, and N_p^{apex} "apex" particles located at each corner of the 2D cluster. Then, $N_p = N_p^{core} + N_p^{edge} + N_p^{apex}$. Upon considering that edge perturbations are attenuated after a single row of nanoparticles (note that, if required, any appropriate factor may be introduced to account for an edge perturbation affecting other rows), one has $N_p^{apex} = 4$ for the *c* arrangement,[15] hence $N_p = N_p^{core} + N_p^{edge} + 4$ (Figure 1c) in which [Eq. (4)]:

$$N_p^{edge} = 4\left(\frac{a_D - 4r_p}{2r_p}\right) = 4\left(\frac{a_D}{2r_p} - 2\right) \tag{4}$$

It is of interest to remark that from Equations (1 and 2), Equation (5):

$$N_p^{edge} = 4\left(\frac{a_D}{2r_p} - 2\right) = 4\left(\frac{a_D}{a_0}\frac{a_0}{2r_p} - 2\right) = 4\left(\sqrt{\frac{N_0}{N_D}} - 2\right) = 4\ (q-2) \tag{5}$$

in which q is defined as a dimensionless parameter characterizing the crystalline quality of the overall arrangement over the whole wafer for a given number N_0 of nanoparticles [Eq. (6)]:

$$q = \sqrt{\frac{N_0}{N_D}} \tag{6}$$

$q = \sqrt{N_0}$ (i.e., $N_D = 1$) represents the perfectly ordered 2D supracrystal that we use as our reference state. Conversely, $q \to 1$ represents the trend towards a full randomization of the nanoparticles (i.e., $N_D \to N_0$).[16] It ensues that with this definition [Eq. (7)]:

$$N_p = \left(\frac{a_D}{2r_p}\right)^2 = \left[\left(\frac{a_D}{a_0}\right)\left(\frac{a_0}{2r_p}\right)\right]^2 = \frac{N_0}{N_D} = q^2 \tag{7}$$

so that[Eq. (8)]:

$$N_p^{core} = N_p - (N_p^{edge} + 4) = \frac{N_0}{N_D} - 4\sqrt{\frac{N_0}{N_D}} + 4 = (q-2)^2 \tag{8}$$

Based on the above considerations, the overall enthalpic change, $\Delta H_{N_D}^{N_0}$, experienced by the system during its transition from the reference state (i.e., $N_D = 1$) to any situation in which $N_D > 1$ is given by the following summation which encompasses all the changes experienced by each particle type of each of the N_D subdomains [Eq. (9)]:

$$\begin{aligned}\Delta H_{N_D}^{N_0} &= (H_{N_D}^{N_0} - H_{N_{D=1}}^{N_0}) \\ &= N_D(N_p^{core}\ H_0^{core} + N_p^{edge}\ H_0^{edge} + 4H_0^{apex}) - N_0 h_0\end{aligned} \tag{9}$$

in which h_0 is the enthalpy per nanoparticle in the reference state (note that h_0 is given by the same expression as the first term of the right-hand side of Equation (9) when imposing $N_D = 1$ and $q = \sqrt{N_0}$). In Equation (9), H_0^j terms represent all the enthalpic contributions experienced by each lattice point of type '*j*' of the array (see Figure 1c).[10] This is defined in the Madelung's sense and accounts for the enthalpic interactions between neighboring particles and with the base substrate, of chemical nature or featuring tension energies incurred by the array or its base substrate surface, including surface tension in/under the subdomain cores or line tensions in/under the boundaries between subdomains. Hence, provided that we focus on N_D values that are not excessively large and N_D ones which are excessively large, H_0^j values may be considered independent of N_D or N_0.

From Equations (5, 7 and 8) it follows that the average enthalpy per particle is [Eq. (10)]:

$$\frac{\Delta H_{N_D}^{N_0}}{N_0} = H_0^{core}\frac{(q-2)^2 + 4(q-2)H_0^{edge}/H_0^{core} + 4\ H_0^{apex}/H_0^{core}}{q^2} - h_0 \tag{10}$$

For simplifying the notations, it is of interest to remark that the "core" enthalpies H_0^{core} are necessarily negative if the overall arrangement presents any stability, whereas H_0^{edge} values are presumably less negative (or even positive) because of the presence of disfavoring interactions prevailing at the edges between perfect 2D clusters. This is certainly even more true for H_0^{apex}. To account for this observation, let us rewrite H_0^{edge} and H_0^{apex} as $H_0^{edge} = H_0^{core}(1-\varepsilon)$ and $H_0^{apex} = H_0^{core}(1-\varepsilon\gamma)$ in which ε is most presumably a positive term and $\gamma \geq 1$ (though the notation and the following analysis remain valid even when this is not the case). Then [Eq. (11)]:

$$\frac{\Delta H_{N_D}^{N_0}}{N_0} = H_0^{core}\left[1 - 4\varepsilon\frac{(q-2)+\gamma}{q^2}\right] - h_0 \tag{11}$$

To assess the relative stability of the overall arrangement vs. the reference state one needs to consider the whole Gibbs energy variation, $\Delta G_{N_D}^{N_0}$, experienced by the array during the transition from $N_D=1$ to $N_D>1$. This includes the entropy variation, $\Delta S_{N_D}^{N_0}$, and not only the enthalpic one. $\Delta S_{N_D}^{N_0}$ is evaluated hereafter upon considering the Boltzmann statistical entropy,[13a] upon considering iso-energetic permutations, i.e., within each type of position: cores, $N_D N_p^{core}$, edges, $N_D N_p^{edge}$, and apexes, $4N_D$. Posing $N_D \Delta S_{N_D}^{N_0} = N_0(k_B S_0)$ in which k_B is the Boltzmann constant and S_0 is a characteristic of the perfect array (hence independent of N_D or of q for a given number, N_0, of nanoparticles), one obtains [Eq. (12)]:[13]

$$\frac{\Delta S_{N_D}^{N_0}}{k_B} = \ln \frac{(N_0)!}{(N_D N_p^{core})!(N_D N_p^{edge})!(4N_D)!} - N_0 s_0 \qquad (12)$$

Finally, since we consider here large numbers of particles of each subtype, we may use the classical approximation $\ln(X!) \approx X \ln X$ in the expression of $\Delta S_{N_D}^{N_0}$ so that [Eq. (13)]:

$$\frac{\Delta S_{N_D}^{N_0}}{k_B N_0} = 2\left\{\ln q - \frac{(q-2)\ln(q-2)}{q} - 2\frac{(q-1)\ln 4}{q^2}\right\} - s_0 \qquad (13)$$

Combining Equations (11 and 13) affords Equation (14):

$$\begin{aligned}\frac{\Delta G_{N_D}^{N_0}}{N_0} = & H_0^{core}\left[1 - 4\varepsilon\frac{(q-2)+\gamma}{q^2}\right] \\ & -2k_B T\left[\ln q - \frac{(q-2)\ln(q-2)}{q} - 2\frac{(q-1)\ln 4}{q^2}\right] \\ & -[h_0 - T(k_B s_0)]\end{aligned} \qquad (14)$$

The term $g_0 = h_0 - T(k_B s_0)$ in the last bracket of Equation (14) is the standard Gibbs free energy per nanoparticle in the reference state so that it is independent of q for a fixed value of N_0. This equation thus establishes that when N_D varies while N_0 is constant (as we consider here), $\Delta G_{N_D}^{N_0}/N_0$ is a function of q being modulated by three parameters, H_0^{core}, ε, γ, which have also constant values. Within this framework, the thermodynamically most stable array is then that corresponding to the value, q^{min}, of q which minimizes $\Delta G_{N_D}^{N_0}/N_0$ when q (i.e., N_D) varies over its possible range.[16] As $\partial^2 \Delta G_{N_D}^{N_0}/\partial q^2 > 0$ over the whole range of possible q values, if any exists, the extremum presented by $\Delta G_{N_D}^{N_0}$ at q^{min} characterizes the Gibbs energy minimum relative to our reference state (defined by $q^{ref} = \sqrt{N_0}$). Thus, q^{min} is the single solution of $\partial(\Delta G_{N_D}^{N_0}/N_0)\partial q = 0$, of Equation (15):

$$\{[q + 2(\gamma-2)]\frac{\varepsilon H_0^{core}}{k_B T} + q\ln(q-2) - (q-2)\ln 4\}_{q=q^{min}} = 0 \qquad (15)$$

q^{min} characterizes the most stable thermodynamic state of the system of N_0 arrayed nanoparticles vs. the perfect array taken as the reference state in this work. Hence, though it characterizes the single local Gibbs energy minimum, it does not at all characterize the propensity of the individual nanoparticles to arrange into this best 2D array, as this depends also on the exact starting conditions characterizing the nanoparticles (or their atomic components) and the substrate before the 2D-supracrystal assembly is made. However, numerous experimental systems have been reported previously to establish that is indeed feasible.[1,2,4–11]

Equation (15) may be solved numerically to afford the variations of q^{min} as a function of $\varepsilon H_0^{core}/k_B T$ for any γ value (see Figure 2). Owing to its definition, γ is a parameter commensurable to unity, so Figure 2 shows that its influence is

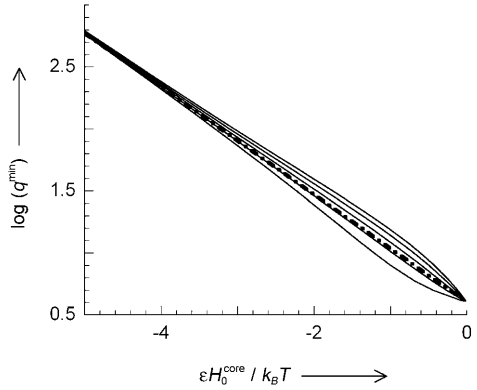

Figure 2. Numerical solution of Equation (15) as a function of $\varepsilon H_0^{core}/k_B T$ and γ for a squared (*c*) configuration (solid curves; from bottom to top: $\gamma = 1,2,3,4$ and 5). The dashed curve is the asymptotic solution given in Equation (17).

very modest and restricted to a range of $|\varepsilon H_0^{core}/k_B T|$ values which are close to unity, i.e., within a range in which q^{min} would be too small to account for any realistic application of the kind envisioned here.[1]

To proceed we may then restrict our analysis to the situations of practical interest,[1] when q is extremely large and $N_0 \gg 1$ as is desired for any realistic applications. Thus, for any case of practical interest here Equation (15) simplifies into Equation (16):

$$\frac{\varepsilon H_0^{core}}{k_B T} + \ln\frac{q^{min}}{4} = 0 \qquad (16)$$

to which the solution is Equation (17):

$$q^{min} = 4\exp\left(-\frac{\varepsilon H_0^{core}}{k_B T}\right) = 4\exp\left(-\frac{H_0^{core} - H_0^{edge}}{k_B T}\right) \qquad (17)$$

This asymptotic analytical solution is superimposed in Figure 2. This establishes the validity of Equation (17) as soon as $|\varepsilon H_0^{core}/k_B T|$ exceeds a few units, i.e., whenever q^{min} reaches any value of practical interest.

It ensues that the most stable *c* arrangement of N_0 particles onto the wafer corresponds to the juxtaposition of N_D^{stable} perfect 2D supracrystals such as Equation (18):

$$N_D^{\text{stable}} = \frac{N_0}{16}\exp\left(2\frac{H_0^{\text{core}} - H_0^{\text{edge}}}{k_B T}\right) \quad (18)$$

To obtain a single 2D supracrystal including all the N_0 nanoparticles, the above value of N_D^{stable} must be at most equal to unity, i.e. Equation (19):

$$\Delta H_0^c = H_0^{\text{core}} - H_0^{\text{edge}} \leq \Delta H_{\max}^c = -\frac{k_B T}{2}\ln\frac{N_0}{16} \quad (19)$$

The condition in Equation (19) shows that the constraint, $H_0^c \leq \Delta H_{\max}^c$, imposed on $\Delta H_0^c = (H_0^{\text{core}} - H_0^{\text{edge}})$ for a *c* lattice results more and more severe when N_0 increases, when the array size increases. Almost identical limits are obtained for arrays involving higher density packings such as squared centered (*cc*) or hexagonal (*hex*) ones (see Appendix) Equation (20):

$$\Delta H_{\max}^{cc} = -\frac{k_B T}{2}\ln\frac{N_0}{8} \quad (20)$$

and Equation (21):

$$\Delta H_{\max}^{hex} = -\frac{k_B T}{2}\ln\frac{N_0}{12} \quad (21)$$

Note that Equations (20 and 21) differ from Equation (19) only by the denominators associated to N_0 in the logarithmic terms of their right-hand sides. As for any macroscopic 2D supracystal these factors are considerably much smaller than N_0, their moderate changes are negligible in the logarithmic values (compare Table 1). In fact the three equations are equivalent to Equation (22):

$$\ln\sqrt{N_0} \approx -\frac{\Delta H_0^{c,\ cc,\ \text{or}\ hex}}{k_B T} \quad (22)$$

Interestingly, this scale law features that irrespective of the lattice type N_0 must be small enough for the positive entropic contribution introduced by the $\sqrt{N_0}$ particles located onto the edges of the perfect single 2D supracrystal to compensate the weak enthalpies and the large negative entropy imposed by the N_0 nanoparticles perfectly arranged within its core. In other terms, the surface area of the supracrystal ($\propto N_0$) must remain small enough for its edges overall length ($\propto \sqrt{N_0}$) to compensate its internal entropic demand.

To illustrate quantitatively the constraints in Equations (19–21), and validate the simplification in Equation (22), Table 1 reports the corresponding threshold values of $\Delta H_{\max}^{c,cc,\ or\ hex}$ for typical sizes of 2D-single crystals composed by nanoparticles of radius of $r_p \approx 1$ nm arranged in each of the three array types. The extremely weak dependence on the type of lattice, even for the smallest supracrystals, validates our point in proposing the general scaling law in Equation (22).

We may particularize further the application of the above scaling law by remarking that upon placing a nanoparticle onto an edge position rather than within the core one cannot impose a too unfavorable enthalpic change since the interactions prevailing in the bulk are already weak. Recognizing that "edge nanoparticles" necessarily experience a loss of stability, owing at least to the absence of half of their neighbors (see, e.g., Figure 1c), one may plausibly assume that ε values fall around $^1/_2$. On the other hand, for most cases reported in the literature up to now,[2,4] average enthalpy per site reaches a few $-k_B T$ at most (i.e., a few times $-2.5\ \text{kJ mol}^{-1}$ or a few mJ m^{-2} at most when expressed in macroscopic units at 300 K).[3] This is required for avoiding the involvement of any strong interactions between particles or with the base substrate which would prevent the sought optical, electronic or magnetic properties.[1] From Table 1 it is then predicted that the maximum expectable size of such arrays lies around a few square micrometers. This predicted range compares extremely well with the largest sizes of defectless areas in 2D supracrystals reported up to date even when crystal growth kinetics seem fully mastered.[2,4]

Conclusion

Though kinetics defects are certainly an important factor that may ultimately limit the size of 2D supracrystals formed by weakly interacting metallic nanoparticles[1–4] it has been shown in this work that a drastic thermodynamic constraint already limits the size of such arrays. Hence, even perfect control of growth kinetics and fast kinetics of defect rearrangements[6–9] cannot solve the problem borne by ordering weakly interacting nanoparticles into large 2D supracrystals except maybe under metastable circumstances. Indeed, a stringent threshold is ultimately imposed by the intrinsic thermodynamics of the system at hand.

This severe condition is ultimately forced onto the system to compensate for the extremely high entropic constraint imposed by a perfect ordering of the 2D-supracrystal elements. Such unfavorable entropic

Table 1. Thermodynamical constraints on $\Delta H_0^{c,\ cc,\ \text{or}\ hex} = (H_0^{\text{core}} - H_0^{\text{edge}})$ for a few selected sizes of 2D-single supracrystals (squared (*c*), centered square (*cc*), or hexagonal (*hex*) lattices) composed of 1 nm radius nanoparticles as a function of the 2D-supracrystal size, as predicted by Equations (19–21).

2D-Single crystal size (a_0)	Number of nanoparticles (N_0)	$\Delta H_{max}^{c,\ cc,\ or\ hex}$ Microscopic units [$k_B T$]			Macroscopic units[a] [kJ mol^{-1}]		
		c	*cc*	*hex*	*c*	*cc*	*hex*
1 cm	2.5×10^{13}	−14.0	−14.4	−14.2	−35	−36	−35
1 mm	2.5×10^{11}	−11.7	−12.1	−11.9	−29	−30	−30
1 μm	2.5×10^{5}	−4.8	−5.2	−5.0	−12	−13	−12

[a] i.e., in *RT* units ($2.5\ \text{kJ mol}^{-1}$ at 300 K); note that for $r_p \approx 1$ nm, $RT \approx 1\ \text{mJ m}^{-2}$ at 300 K (compare with ref. [3]).

demand may be easily compensated in crystals involving large negative enthalpies, but results especially difficult to balance by weak enthalpies of interaction between the nanoparticles. Hence, it may be relaxed only by the introduction of enough disorder in the array, by considering sufficiently small crystals so that their edge length ($\propto\sqrt{N_0}$) is comparatively large enough vs. its surface area ($\propto\sqrt{N_0}$).

We have evaluated the thermodynamics of the system for a coverage of 2D supracrystals composed of nanoparticles arranged in three typical lattices (*c*, *cc*, and *hex*). The very similar results obtained for *c*, *cc*, or *hex* arrangements establish that the exact crystallographic structure has minimal influence whenever N_0 is extremely large as expected for realistic devices.[1] Therefore the principle of the present approach and, most importantly, its general outcome in the form of the scaling law in Equation (22) appear to be readily transposable to almost any other realistic crystalline 2D configuration whenever the defects may aggregate to form one-dimensional domains limiting perfect 2D domains.

This clearly evidences that perfect kinetic control is not sufficient for allowing large 2D supracrystals of weakly interacting objects to be grown.[1] Thus, new synthetic strategies must be developed to achieve supracrystals ordering over surface areas which may lead to industrial applications.[17]

It is also of interest to consider that the same concept may certainly be transposed to 3D networks. Indeed, in such a case the number of ordered objects, N_0, to be arranged grows as the cube of the crystal size (vs. growing as its square for a 2D network) while those on its surface grow as its square (as $\propto N_0^{2/3}$ instead of $\propto N_0^{1/2}$ for a 2D network). This may impose different, but still stringent conditions onto the size of single 3D crystals which may be obtained from weakly interacting objects (large organic molecules, proteins, etc.), as is frequently observed when single crystals are grown for X-ray structural analyses. Therefore the present approach may serve as a qualitative basis for explaining the great difficulties experienced in obtaining even micrometric single crystals from these objects.

To conclude, we wish to recall that the scaling law concept developed here is somewhat akin to that introduced by P. G. de Gennes in his "blob theory" to predict the statistical conformation of long polymers and polyelectrolytes in solution.[18] Though the exact rationales and physicochemical areas are different, the concepts underlying the two models and their outcomes in terms of thermodynamically favored structures have similar roots. Indeed, both find ultimately their origin in the fact that in ordered systems entropic demands grow faster than enthalpic ones when the number of arrayed elements increases. Therefore, the trend to fragment into subdomains is to be considered as a natural outcome which becomes especially visible for systems involving weak interaction enthalpies as it is the case for 2D arrays of weakly interacting nanoparticles, 3D crystals of organic and biological molecules, as well as long chains of polymers or polyelectrolytes.

Appendix

Thermodynamical threshold for 2D supracrystals with higher density packings: For the sake of simplicity in the intermediate derivations, in the main text we purposely considered 2D-squared arrays, as for these lattices the accounting of edge, apex, and core particles is the simplest, although bearing intact the essential factors and attributes that control the validity of our scaling law. Yet as expressed in the Introduction, higher-density packings such as hexagonal or squared-centered arrays are generally spontaneously preferred in real 2D-supra lattices of nanoparticles.

It is the purpose of this Appendix to disclose the results for these higher density 2D packings and to justify our statement about the generality of the laws disclosed above provided that geometrical factors commensurable to unity are taken into account according to the specificity of the 2D packing. We use hereafter the same notations as in the main text.

For the centered square (*cc*) packing, the values of N_0, N_D, N_p and N_p^{apex} given in Equations (1–3) for a *c* lattice remain identical. The difference between simple squared and centered squared arrays reveals only in N_p^{apex}, owing to the change in compactness. Thus, upon the introduction of the crystalline quality parameter $q=\sqrt{N_0/N_D}$ [Eq. (6)], one obtains now [Eq. (23)]:

$$(N_p^{edge})^{cc}=4\left(\frac{a_D}{2\sqrt{2}r_p}-2\right)=4\left(\frac{q}{\sqrt{2}}-2\right) \tag{23}$$

and, noting that [Eq. (24)]

$$(N_p)^{cc}=q^2 \tag{24}$$

one obtains [Eq. (25)]:

$$(N_p^{core})^{cc}=(N_p)^{cc}-[(N_p^{edge})^{cc}+4]=q^2-2\sqrt{2}q+4=(q-\sqrt{2})^2+2 \tag{25}$$

instead of Equations (5,7, and 8). Based on these definitions, one finally obtains the counterparts of Equations (11 and 13) for a squared centered 2D supracrystal [Eq. (26)]:

$$\left(\frac{\Delta H_{N_D}^{N_0}}{N_0}\right)^{cc}=H_0^{core}\left[1-2\varepsilon\frac{\sqrt{2}q+2(\gamma-2)}{q^2}\right]-h_0 \tag{26}$$

and [Eq. (27)]:

$$\begin{aligned}\left(\frac{\Delta S_{N_D}^{N_0}}{k_B N_0}\right)^{cc}=&2\ln q-\frac{(q-\sqrt{2})^2+2}{q^2}\ln[(q-\sqrt{2})^2+2]\\&-\frac{2\sqrt{2}q-8}{q^2}\ln[2\sqrt{2}q-8]-\frac{4}{q^2}\ln 4-s_0\end{aligned} \tag{27}$$

For a hexagonal array, considering now that a_0 is the side length of a macroscopic hexagonal substrate (instead of a squared one as in Figure 1a), one obtains [Eq. (28)]:

$$(N_0)^{hex}=3\left(\frac{a_0}{2r_p}\right)^2-3\frac{a_0}{2r_p}+1\underset{a_0\gg r_p}{\longrightarrow}3\left(\frac{a_0}{2r_p}\right)^2 \tag{28}$$

in which the limit in the right-hand-side is achieved when a_0 is considerably large compared to the nanoparticles sizes. Similarly, one has [Eq. (29)]:

$$(N_D)^{hex}=\frac{A_0}{A_D}=\frac{\frac{3\sqrt{3}}{2}a_0{}^2}{\frac{3\sqrt{3}}{2}a_D{}^2}=\left(\frac{a_0}{a_D}\right)^2 \tag{29}$$

and [Eq. (30)]:

$$(N_p)^{hex} = 3\left(\frac{a_D}{2r_p}\right)^2 - 3\frac{a_D}{2r_p} + 1 \xrightarrow[a_0 \gg r_p]{} 3\left(\frac{a_D}{2r_p}\right)^2 \tag{30}$$

so that upon remarking that $N_p^{apex} = 6$ for hexagonal packing, so that $N_p = N_p^{core} + N_p^{edge} + 6$, the counterpart of Equation (5) is [Eq. (31)]:

$$(N_p^{edge})^{hex} = 6\left(\frac{a_D}{2r_p} - 2\right) \tag{31}$$

Introducing the crystalline quality parameter $q = \sqrt{N_0/N_D}$ [Eq. (6)], and noting that [Eq. (32)]:

$$(N_p)^{hex} = q^2 \tag{32}$$

finally allows to express the counterparts of Equations (5 and 8) for a 2D-hexagonal packing [Eq. (33)]:

$$\begin{aligned}(N_p^{edge})^{hex} = 6\left(\frac{a_D}{2r_p} - 2\right) = 6\left(\frac{a_D}{a_0}\frac{a_0}{2r_p} - 2\right) &= 6\left(\frac{1}{\sqrt{3}}\sqrt{\frac{N_0}{N_D}} - 2\right) \\ &= 6\left(\frac{1}{\sqrt{3}}q - 2\right)\end{aligned} \tag{33}$$

and [Eq. (34)]:

$$(N_p^{core})^{hex} = (N_p)^{hex} - [(N_p^{edge})^{hex} + 6] = q^2 - 2\sqrt{3}q + 6 = (q - \sqrt{3})^2 + 3 \tag{34}$$

Thus, one obtains finally the enthalpy per particle [Eq. (35)]:

$$\left(\frac{\Delta H_{N_D}^{N_0}}{N_0}\right)^{hex} = H_0^{core}\left[1 - 2\varepsilon\frac{\sqrt{3}q + 3(\gamma - 2)}{q^2}\right] - h_0 \tag{35}$$

and the corresponding Boltzmann entropic contribution [Eq. (36)]:

$$\begin{aligned}\left(\frac{\Delta S_{N_D}^{N_0}}{k_B N_0}\right)^{hex} &= 2\ln q - \frac{(q - \sqrt{3})^2 + 3}{q^2}\ln[(q - \sqrt{3})^2 + 3] \\ &\quad - \frac{2\sqrt{3}q - 12}{q^2}\ln[2\sqrt{3}q - 12] - \frac{6}{q^2}\ln 6 - s_0\end{aligned} \tag{36}$$

Based on the above derivations for squared centered [Eqs. (26 and 27)] or hexagonal [Eqs. (35 and 36)] arrays, one may readily evaluate the corresponding values q^{min} which minimize the standard Gibbs free energies of each type of lattice. These are shown graphically in Figure 3 as a function of $\varepsilon H_0^{core}/k_B T$ for different values of γ as was performed above for simple squared arrays (compare Figure 2). It is again observed that for arrays of sizes which are relevant to our purpose here, when q^{min} is not much less than $\sqrt{N_0}$, its dependence on $\varepsilon H_0^{core}/k_B T$ becomes asymptotically independent of γ. The corresponding asymptotic limits are readily evaluated through the same procedure as that disclosed in detail in the main text for simple squared arrays. This affords the counterparts of Equation (17) for centered squared arrays of sufficiently large sizes (such as q^{min} be comparable to $\sqrt{N_0}$) [Eq. (37)]:

$$q^{min} = 2\sqrt{2}\exp\left(-\frac{\varepsilon H_0^{core}}{k_B T}\right) = 2\sqrt{2}\exp\left(-\frac{H_0^{core} - H_0^{edge}}{k_B T}\right) \tag{37}$$

or for hexagonal ones under the same conditions [Eq. (38)]:

$$q^{min} = 2\sqrt{3}\exp\left(-\frac{\varepsilon H_0^{core}}{k_B T}\right) = 2\sqrt{3}\exp\left(-\frac{H_0^{core} - H_0^{edge}}{k_B T}\right) \tag{38}$$

Note that, as stated in the Introduction, the exact crystallographic nature of the 2D supracrystal shows up only through small variations in the numerical factors of the exponential terms: indeed, the factor 4 in Equation (17) is now replaced by $2\sqrt{2} \approx 2.8$ or $2\sqrt{3} \approx 3.5$ respectively for the squared centered or the hexagonal cases. Equations (37 and 38) show that the values of N_D^{stable}, which characterize the most stable number of clusters when N_0 particles are arranged onto the wafer in each case are

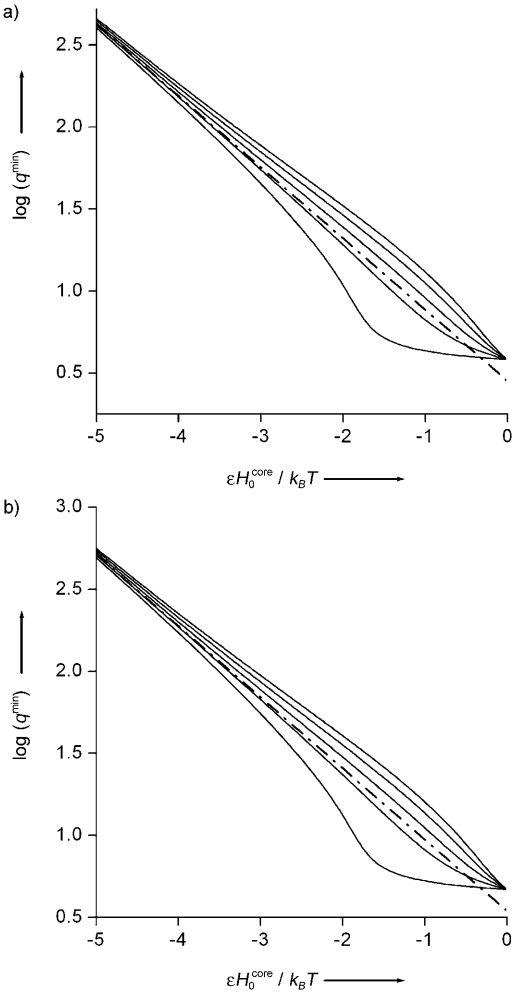

Figure 3. Variations of q_{min} as a function of $\varepsilon H_0^{core}/k_B T$ and γ (solid curves; from bottom to top: $\gamma = 1,2,3,4$ and 5) for a) centered square arrangement, or b) for a hexagonal one. The dashed lines in (a, b) are the asymptotic solutions given in Equations (37 or 38), respectively.

[compare with Equation (18)] [Eq. (39)]:

$$N_D^{stable} = \frac{N_0}{8}\exp\left(2\frac{H_0^{core} - H_0^{edge}}{k_B T}\right) \tag{39}$$

for a squared-centered configuration and [Eq. (40)]:

$$N_D^{stable} = \frac{N_0}{12}\exp\left(2\frac{H_0^{core} - H_0^{edge}}{k_B T}\right) \tag{40}$$

for a hexagonal one. It ensues that in order to obtain a single 2D supracrystal involving all the N_0 nanoparticles onto the wafer ($N_D^{stable} \leq 1$) the following conditions must be fulfilled [Eq. (41)]:

$$(H_0^{core} - H_0^{edge})^{cc} \leq (H_0^{core} - H_0^{edge})_{max}^{cc} = -\frac{k_B T}{2}\ln\frac{N_0}{8} \tag{41}$$

for a square centered array or [Eq. (42)]:

$$(H_0^{core} - H_0^{edge})^{hex} \leq (H_0^{core} - H_0^{edge})_{max}^{hex} = -\frac{k_B T}{2}\ln\frac{N_0}{12} \tag{42}$$

for a hexagonal one [compare with Equation (19)]. These conditions correspond respectively to Equations (20 and 21) reported in the main text.

Acknowledgements

This work was supported in parts by CNRS (UMR 8640 "PASTEUR" and LIA "XiamENS"), Ecole Normale Supérieure (ENS), Université Pierre et Marie Curie (UPMC), and by the French Ministry of Research.

[1] M. Brust, *Nat. Mater.* **2005**, *4*, 364–365.

[2] a) A. Taleb, C. Petit, M. P. Pileni, *J. Phys. Chem. B* **1998**, *102*, 2214–2220; b) M. P. Pileni, *J. Phys. Chem. B* **2001**, *105*, 3358–3371; c) L. Motte, F. Billoudet, M. P. Pileni, *J. Phys. Chem.* **1995**, *99*, 16425–16429; d) Y. Lalatonne, J. Richardi, M. P. Pileni, *Nat. Mater.* **2004**, *3*, 121–125; e) M. P. Pileni, Y. Lalatonne, D. Ingert, I. Lisiecki, A. Couty, *Faraday Discuss.* **2004**, *3*, 251–264; f) A. Couty, A. Mermet, P. A. Albouy, E. Duval, M. P. Pileni, *Nat. Mater.* **2005**, *4*, 395–398; g) X. Zhang, B. Sun, R. H. Friend, H. Guo, D. Nau, H. Giessen, *Nano Lett.* **2006**, *6*, 651–655; h) A. Courty, A. I. Henry, N. Goubet, M. P. Pileni, *Nat. Mater.* **2007**, *6*, 900–907; i) M. P. Pileni, *J. Phys. Chem. C* **2007**, *111*, 9019–9038; M. P. Pileni, *Acc. Chem. Res.* **2007**, *40*, 685–693.

[3] A. S. Eppler, G. Rupprechter, E. A. Anderson, G. A. Somorjai, *J. Phys. Chem.B* **2000**, *104*, 7286–7292.

[4] a) C. P. Collier, R. J. Saykally, J. J. Shiang, S. E. Heinrichs, J. R. Heath, *Science* **1997**, *277*, 1978–1981; b) I. S. Weitz, J. L. Sample, R. Ries, E. M. Spain, J. R. Heath, *J. Phys. Chem. B* **2000**, *104*, 4288–4291; c) B. M. Quinn, I. Prieto, S. K. Haram, A. J. Bard, *J. Phys. Chem. B* **2001**, *105*, 7474–7476; d) M. A. El-Sayed, *Acc. Chem. Res.* **2001**, *34*, 257–264; e) X. Xu, G. Friedman, K. D. Humfeld, S. A. Majetich, S. A. Asher, *Chem. Mater.* **2002**, *14*, 1249–1256; f) C. Chapon, S. Granjeaud, A. Humbert, C. R. Henry, *Eur. Phys. J.* D **2001**, *13*, 23–30; g) C. Lopez, *Adv. Mater.* **2003**, *15*, 1679–1704; h) P. A. Kossyrev, A. Yin, S. G. Cloutier, D. A. Cardimona, D. Huang, P. M. Alsing, J. M. Xu, *Nano Lett.* **2005**, *5*, 1978–1981.

[5] a) C. B. Murray, C. R. Kagan, M. G. Bawendi, *Science* **1995**, *270*, 1335–1338; b) A. Taleb, C. Petit, M. P. Pileni, *Chem. Mater.* **1997**, *9*, 950–959; c) J. Tanori; M. P. Pileni, *Langmuir* **1997**, *13*, 639–646; d) M. P. Pileni, *Langmuir* **1997**, *13*, 3266–3276; e) M. P. Pileni, *Nature Mater.* **2003**, *2*, 145–150; f) D. Vollath, D. V. Szabo, R. D. Taylor, J. O. Willis, *J. Mater. Res.* **1997**, *12*, 2175–2182; g) K. M. Sung, D. W. Mosley, B. R. Peelle, S. Zhang, J. M. Jacobson, *J. Am. Chem. Soc.* **2004**, *126*, 5064–5065; h) M. Okuda, Y. Kobayashi, K. Suzuki, K. Sonoda, T. Kondoh, A. Wagawa, H. Yoshimura, *Nano. Lett.* **2005**, *5*, 991–993; i) R. A. McMillan, J. Howard, N. J. Zaluzec, H. K. Kagawa, R. Mogul, Y. F. Li, C. D. Paavola, J. D. Trent, *J. Am. Chem. Soc.* **2005**, *127*, 2800–2801.

[6] a) C. Harrison, D. E. Angelescu, M. Trawick, Z. Cheng, D. A. Huse, P. M. Chaikin, D. A. Vega, J. M. Sebastian, R. A. Register, D. H. Adamson, *Europhys. Lett.* **2004**, *67*, 800–806; b) J. Vedrine, Y.-R. Hong, A. P. Marencic, R. A. Register, D. H. Adamson, P. M. Chaikin, *Appl. Phys. Lett.* **2007**, *91*, 143110; c) A. P. Marencic, M. W. Wu, R. A. Register, P. M. Chaikin, *Macromol.* **2007**, *40*, 7299–7305.

[7] a) M. R. Hammond, S. W. Sides, G. H. Fredrickson, E. J. Kramer, J. Ruokolainen, S. F. Hahn, *Macromol.* **2003**, *36*, 8712–8716; b) E. J. Kramer, *Nature* **2005**, *437*, 824–825; c) J. J. Chiu, B. J. Kim, G.-R. Yi, J. Bang, E. J. Kramer, D. J. Pine, *Macromol.* **2007**, *40*, 3361–3365; d) G. E. Stein, E. J. Kramer, X. Li, J. Wang, *Phys. Rev. Lett.* **2007**, *98*, art. no. 086101; e) G. E. Stein, E. W. Cochran, K. Katsov, G. H. Fredrickson, E. J. Kramer, X. Li, J. Wang, *Phys. Rev. Lett.* **2007**, *98*, art. no. 158302.

[8] a) D. R. Nelson, B. I. Halperin, *Phys. Rev. B* **1979**, *19*, 2457–2484; b) D. R. Nelson, B. I. Halperin, *Science* **1985**, *229*, 233–238; c) P. Lipowsky, M. J. Bowick, J. H. Meinke, D. R. Nelson, A. R. Bausch, *Nat. Mater.* **2005**, *4*, 407–411; d) M. J. Bowick, A. Cacciuto, D. R. Nelson, A. Travesset, *Phys. Rev. B* **2006**, *73*, 1–16; e) V. Vitelli, J. B. Lucks, D. R. Nelson, *Proc. Nat. Acad. Sc. USA*, **2006**, *103*, 12323–12328; f) M. J. Bowick, D. R. Nelson, H. Shin, *Phys. Chem. Chem. Phys.* **2007**, *9*, 6304–6312.

[9] See the Gerhard Ertl's Nobel Lecture: G. Ertl, *Angew. Chem.* **2008**, *120*, 3578–3590; *Angew. Chem. Int. Ed.* **2008**, *47*, 3524–3535.

[10] M. M. Maye, W. Zheng, F. L. Leibowitz, N. K. Ly, C. J. Zhong, *Langmuir* **2000**, *16*, 490–497.

[11] a) D. R. Nelson, L. Peliti, *J. Phys. (Paris)* **1987**, *48*, 1085–1092; b) R. Radhakrishnan, K. E. Gubbins, M. Sliwinska-Bartkowiak, *Phys. Rev. Lett.* **2002**, *89*, art. no. 07101.

[12] K. Saito, Y. Yamamura, *Thermochim. Acta* **2005**, *431*, 21–23.

[13] a) P. Atkins, J. de Paula, *Physical Chemistry*, 8th ed., Oxford Univ. Press, Oxford, **2006**; b) Note that in Equation (12) we do not consider the permutation of the clusters themselves ($(N_D)!$) because exchanging all particles within their domains and between domains at constant energetic levels as formulated in Equation (12) already involves this entropic contribution.

[14] Dislocations separating subdomains have necessarily a width. Hence their creation into an initially perfect 2D supracrystal necessarily increases the surface area of the supracrystal, and hence modifies the base substrate surface tension. However, on the one hand this may be included into the edge enthalpy considered here. On the other hand, as we are interested in systems such as $N_D \rightarrow 1$ and with non-fractal boundaries, the resulting variation, ΔA_0, in the surface area of the 2D supracrystal is proportional to $r_p d\sqrt{N_0}$ in which d is the average width of a boundary while the surface area, A_0, of the crystal is proportional to $r_p^2 N_0$. Thus, provided that N_0 is large enough and d is at most in the same range as the nanoparticle size, r_p, one has $\Delta A_0/A_0 \propto 1/\sqrt{N_0} \rightarrow 0$. These conditions correspond perfectly to the systems which are actually produced experimentally.[2–4] Hence the ensuing variations in substrate surface tension may be neglected in our analysis.

[15] Note that the very crystallographic nature of a supracrystal will intervene in our analysis only by specifying the numerical factors which give the exact relationships between N_0, N_D and N_p on the one hand and a_0, a_D, and r_p, on the other hand. As evidenced in the Appendix, adapting the present analysis to different supracrystals requires that N_0, N_D, N_p and ω_a are specific parameters close to unity, as evidenced in the Appendix for squared centered or hexagonal arrays.

[16] Note that from the definition in Equation (6) one would deduce that: $1 \le q \le \sqrt{N_0}$. However, the requirement about 4 apexes in each cluster (Figure 1c) for a squared (*c*) or squared centered (*cc*) configurations imposes that the largest N_D value is equal to $N_0/4$, hence $2 \le q \le \sqrt{N_0}$. For hexagonal (*hex*) lattices, there are 6 apexes, hence $6 \le q \le \sqrt{N_0}$. However since $q > 1$ for the systems of practical interest the exact values of the lower limits of the q range are irrelevant to our analyses.

[17] One possible approach to overcome the dual constraint between i) strong enthalpic interactions with the array lattice nodes and ii) weak enthalpic interactions between the elements of the array is to uncouple chemically both constraints. For example, the nanoparticles may be linked to the 2D surface through strong covalent bonds quantically uncoupled from the nanoparticles. See, e.g.: K. Bandyopadhyay, V. Patil, K. Vijayamohanan, M. Sastry, *Langmuir* **1997**, *13*, 5244–5248.

[18] a) P. G. de Gennes, *Makromol. Chem.* **1979**, *3*, 195–196. For comments about the importance of de Gennes's "Blob Theory" see, e.g.: b) J. S. Higgins, *Polym. Int.* **1992**, *27*, 295–296; c) F. Brochard-Wyart, *Nature* **2007**, *448*, 149; d) A. Ajdari. , *Science* **2007**, *317*, 466.

Received: June 3, 2008
Published online: August 7, 2008

